0026-895X/94/061242-11$03.00/0

MOLECULAR PHARMACOLOGY, 45:1242-1252, 1994.

Aminopyridine Block of Kv1.1 Potassium Channels Expressed in Mammalian Cells and *Xenopus* Oocytes

NEIL A. CASTLE, SANDRA FADOUS, DIOMEDES E. LOGOTHETIS,[1] and GING KUO WANG

Department of Anesthesia Research Laboratories, Brigham and Women's Hospital (N.A.C., S.F., G.K.W.), and Howard Hughes Medical Institute, Department of Cardiology, Children's Hospital Medical Center, and Departments of Pediatrics and Cellular and Molecular Physiology (D.E.L.), Harvard Medical School, Boston, Massachusetts 02115

Received January 3, 1994; Accepted March 23, 1994

SUMMARY

The mechanism by which aminopyridines (APs) block cloned Kv1.1 K^+ channels expressed either in the mammalian Sol-8 muscle cell line or in *Xenopus* oocytes was investigated using whole-cell patch-clamp and two-electrode voltage-clamp techniques. When Sol-8 cells were exposed to 4-AP (30 μM to 1 mM) or 3-AP (300 μM to 10 mM) for 1–2 min at a holding potential of −80 mV, delayed rectifier K^+ currents activated by the first depolarization to +40 mV showed a small reduction in peak amplitude but exhibited a rapid decay phase that was absent in control records. However, currents elicited by subsequent pulses showed maximal block throughout the pulse. These results suggest that 4-AP requires the channel to be activated before block can occur readily. After a 10-min washout of 4-AP in the absence of channel activation, the current elicited at the beginning of the first depolarizing pulse was similar to that observed during maximal block. However, during the pulse the current increased in an exponential manner, to an amplitude similar to that seen in the absence of 4-AP. Subsequent pulses elicited currents with profiles similar to that observed in controls. These results suggest that channel activation is also required for unblock (i.e., 4-AP is trapped when the channel closes). Block of Kv1.1 channels by 4-AP was voltage dependent. The magnitude of block decreased progressively as the membrane potential was depolarized to voltages more positive than −20 mV. The concentration producing half-maximal inhibition (IC_{50}) of Kv1.1 currents in Sol-8 cells at +40 mV at physiological pH (7.2) was 89 μM for 4-AP (pK_a = 9.2) and 2.2 mM for 3-AP (pK_a = 6.0). However, when the intracellular pH was lowered to 6.0 the IC_{50} for 3-AP decreased to 290 μM. These results are consistent with the charged form of the APs being the active species.

APs have been shown to block voltage-activated potassium channels in a variety of cell types, including neurons (1, 2), skeletal muscle cells (3), cardiac muscle cells (4–6), secretory cells (7), and cells of the immune system (8). A number of early studies examining 4-AP block of delayed rectifier currents in nerve axons showed that inhibition was relieved by prolonged membrane depolarization or by increases in the frequency of short depolarizations (2, 9). These findings resulted in the proposal that 4-AP blocks closed or resting K^+ channels (2). A similar mechanism has been proposed to underlie 4-AP inhibition of voltage-dependent transient outward K^+ currents in molluscan neurons (10), mammalian melanotrophs (7), and cardiac muscle cells (4–6). However, several studies have provided evidence that 4-AP inhibition of some transient outward K^+ channels is better described by a preferential block of the open state of the channel (8, 11). In a recent study examining the cloned K^+ channels Kv2.1 and Kv3.1, 4-AP was proposed to produce block by interacting with open and closed channels (12).

In the present study we have characterized 4-AP block of the cloned delayed rectifier K^+ channel Kv1.1 in transfected Sol-8 cells (13) and in *Xenopus* oocytes injected with cRNA. Although several studies have shown that this channel is blocked by 4-AP (14–16), the mechanism underlying the inhibition has not been determined. The results presented in this study lead us to conclude that 4-AP block of Kv1.1 K^+ channels requires channel activation. Furthermore, 4-AP can be trapped within the channel at hyperpolarized potentials. This suggests that the channel must be activated for 4-AP to unblock. A preliminary report of some of this work has appeared in abstract form (17).

Materials and Methods

Preparation of Sol-8 cells. Sol-8 cells stably transfected with Kv1.1 (RCK1) K^+ channel cDNA (13) were used in this study. Cells

This work was supported by funds from the Brigham and Women's Hospital Anesthesia Foundation (to N.A.C.), National Institutes of Health Biomedical Research Support Grant BRSG S07 RR0595007 (to N.A.C.), National Institutes of Health Grant GM35401 (to G.K.W.), and National Institutes of Health Grant HL46383 (to D.E.L.).

[1] Present address: Department of Physiology and Biophysics, Mount Sinai School of Medicine, New York, NY 10029–6574.

ABBREVIATIONS: AP, aminopyridine; HEPES, 4-(2-hydroxyethyl)-1-piperazineethanesulfonic acid; EGTA, ethylene glycol bis(β-aminoethyl ether)-*N*,*N*,*N*′,*N*′-tetraacetic acid.

were maintained in culture in Dulbecco's modified Eagle medium, supplemented with 20% heat-inactivated fetal calf serum and 0.6 mg/ml G418 (geneticin) (GIBCO Laboratories, Grand Island, NY), at 37° in a humidified atmosphere containing 5% CO_2. The geneticin was present as a selection factor for cells containing the Kv1.1 cDNA. The culture medium was changed every 3–4 days. Once each week, the cells were detached from the culture flask with pancreatin (GIBCO Laboratories) made in phosphate-buffered saline. Some of the cells were replated onto 35-mm plastic Petri dishes (Falcon Plastics, Cockeysville, MD) containing the supplemented Dulbecco's modified Eagle medium plus 50 or 100 μM $ZnCl_2$. Zinc was included to enhance the transcription of Kv1.1 cDNA via an augmentation of the metallothionine-1 promoter present in the expression plasmid. In contrast to the observations of Koren *et al.* (13), expression of Kv1.1 currents in the absence of zinc was only infrequently observed. Cells were used for electrophysiology 2–4 days after plating.

***Xenopus* oocyte preparation.** Under anesthesia, ovarian lobes were surgically removed. Oocytes were subjected to digestion for 20 min in a nominally Ca^{2+}-free medium containing 2 mg/ml collagenase. The oocytes were then defolliculated manually. Defolliculated oocytes were stored overnight at 17°. Viable oocytes were then injected with 50 nl of mRNA (1 mg/ml) via a glass micropipette (diameter, 15–25 μm). mRNA was prepared as described previously by Koren *et al.* (13). Injected oocytes were stored at 17° for up to 5 days in modified Barths's solution containing (in mM) 88 NaCl, 1 KCl, 2.4 $NaHCO_3$, 0.82 $MgCl_2$, 0.33 $Ca(NO_3)_2$, and 0.41 $CaCl_2$.

Electrophysiology. Much of the present study was performed on Sol-8 cells; however, we also examined the actions of APs on Kv1.1 channels expressed in *Xenopus* oocytes. Although Sol-8 cells have the advantage of being small and thus the time course for onset and washout of drug effects is relatively rapid (~2 min for onset and ~10 min for washout at 1 mM 4-AP, compared with ~10 min for onset and >90 min for washout in oocytes), oocytes were found to be more robust. It was possible to maintain electrophysiological recording in oocytes for several hours, which was sometimes necessary for some of the voltage-clamp protocols used in this study. Furthermore, unlike Sol-8 cells, oocytes remained stable during large membrane depolarizations (i.e., up to +140 mV).

Two-electrode voltage-clamp of oocytes. For recordings, oocytes were transferred into a chamber that was continuously superfused at 1.25 ml/min with a recording solution containing (in mM), 120 NaCl, 5.4 KCl, 0.3 $CaCl_2$, 1 $MgCl_2$, and 10 HEPES, pH 7.2. Currents were measured using a conventional two-electrode voltage-clamp amplifier (Warner OC-725; Warner Instrument Corp., Hamden, CT). Creation of voltage-clamp pulses was controlled by pCLAMP software (Axon Instruments, Foster City, CA) interfaced to the amplifier via a 125-kHz Labmaster board. Microelectrodes were filled with 3 M KCl and had resistances of 0.5–1.0 MΩ. Drugs were applied to the oocytes by exchanging the entire bathing solution via gravity-fed reservoirs. All experiments were performed at room temperature (~23°).

Whole-cell voltage-clamp of Sol-8 cells. The whole-cell variant of the patch-clamp technique (18) was used to measure voltage-dependent K^+ currents in Sol-8 cells. Before each experiment, the culture medium was replaced with an extracellular bathing solution containing (in mM) 145 NaCl, 5.4 KCl, 2 $CaCl_2$, 2 $MgCl_2$, and 10 HEPES, adjusted to pH 7.5 with NaOH. The dish containing the transfected Sol-8 cells was mounted on the stage of an inverted microscope and continuously perfused with the external bathing solution at a flow rate of 2 ml/min.

Recording micropipettes were fabricated from borosilicate capillary tubing (Boralex, Rochester, NY) and had tip resistances of 1–2 MΩ when filled with an intracellular fluid-like solution. In the present study two different intracellular solutions were used. Solution 1 contained (in mM) 145 KCl, 3 mM magnesium ATP, 10 EGTA, and 10 HEPES, adjusted to pH 7.2 with KOH. Solution 2 contained (in mM) 100 KF, 45 KCl, 10 EGTA, and 10 HEPES, adjusted to pH 7.2 with KOH. The outward currents measured using the two micropipette solutions exhibited similar characteristics. However, it was found that seal stability was much greater with solution 2. Therefore, solution 2 was used in the majority of experiments.

Voltage-clamp was achieved using an EPC-7 patch-clamp amplifier (Adams and List Associates, Great Neck, NY). Creation of voltage-clamp pulses and data acquisition were controlled by pCLAMP software interfaced to the amplifier via a 125-kHz Labmaster board. Except where noted, cells were maintained at a holding potential of −80 mV between pulse protocols. Capacitive currents were partially compensated using analog circuitry, with the remainder being canceled along with leakage currents using an inverted and scaled average of five hyperpolarizing pulses one fifth the magnitude of the depolarizing pulse, delivered from a subtraction holding potential of −80 mV.

APs were applied to individual cells via a series of narrow bored capillary tubes (inner diameter, ~100 μm; Drummond Scientific Co. Broomall, PA) positioned within 200 μm of the cell under examination. Drugs were made up in the extracellular solution. All drug responses were compared with records obtained with control solution flowing out of one of the tubes.

A consistent observation during voltage-clamp experiments was that, upon establishment of the whole-cell configuration, a 2–10-fold increase in the amplitude of the voltage-dependent outward current developed over a period of 10 min. The current then remained relatively constant at this level for up to 1 hr. This current "run-up" was observed with both internal solutions 1 and 2, suggesting that ATP was not required for this phenomenon. It is possible that an intracellular factor is dialyzed out of the cell after the establishment of the whole-cell configuration. Another possibility is the zinc that presumably accumulates within the cell during culture. Zinc at micromolar concentrations has been shown to inhibit a number of ion channels when applied extracellularly (19–21) and has been proposed to inhibit Ca^{2+}-dependent K^+ channels in hippocampal neurons via an intracellular mechanism (22). A clearer explanation for the run-up phenomenon will require further study.

In addition to the expression of Kv1.1 K^+ currents, Sol-8 cells were found to express a voltage-dependent sodium current and a time-independent outward rectifying current. The sodium current was observed only when cell density was high (>70% confluent). The time-independent outward current was present in all cells and exhibited run-up after the establishment of the whole-cell configuration. However, unlike Kv1.1 K^+ currents, the time-independent current exhibited subsequent "run-down" and usually disappeared within 10–20 min of establishment of the whole-cell mode. Before run-down this current contributed at most 15% of the total outward current. After run-down the contribution of this current was not measurable in 80% of cells and did not exceed 5% in the remainder of the cells. The current is probably carried by chloride ions, because replacement of extracellular Cl^- by aspartate resulted in a reversal of current direction at +40 mV (internal solution 2 was used). To reduce the contamination of voltage-activated outward currents with this time-independent current, measurement of currents was usually started 15 min after the establishment of the whole-cell configuration. The time-independent current was not affected by 3 mM 4-AP (highest concentration used in this study).

The amplitude of voltage-dependent outward currents in Sol-8 cells was found to be large, ranging from 1 nA to 18.5 nA at +40 mV. The median current amplitude of the cells used in this study was 5.5 nA at +40 mV (mean, 6.7 ± 0.4 nA; n = 85 cells). For quantitative analyses (i.e., dose-respose curves and voltage dependences), cells with current ampltitudes of <6 nA were used. After series resistance compensation (~70%), the estimated maximal voltage drop across the pipette tip using these cells did not exceed 7 mV. Our estimate of the maximal voltage offset was based on estimates of the access resistance of the whole-cell configuration, determined in a standard manner by measuring both the time constant of decay and the integral of the capacitative current transient elicited by a 10-mV voltage step from a holding potential of −80 mV (current was filtered at 10 kHz and sampled at 100 kHz). The mean time constant for decay of the capacitative current was 130 ± 26 μsec (n = 10) and cell capacitance was 35.7 ± 5.2 pF

($n = 10$) [comparable to 32 pF reported by Koren *et al.* (13)]. The mean uncompensated access resistance estimated from $\tau_{C_{sp}}/C$ for individual cells was 3.8 ± 0.5 MΩ. With 70% series resistance compensation the remaining uncompensated access resistance was estimated to be 1.1 MΩ. Although a maximal voltage drop of 7 mV does not effect the qualitative nature of the results presented in this study, it is sufficiently large to prevent us from providing precise analyses of features such as the voltage dependence of 4-AP block. Some cells expressing currents greater than 10 nA have been used to illustrate qualitative aspects of AP interaction with Kv1.1 channels.

Chemicals. 4-AP and 3-AP were purchased from Sigma Chemical Co. (St. Louis, MO). 4-AP was made up as a 1 M stock solution containing, in addition, 100 mM HEPES and adjusted to pH 7.5 with NaOH. 3-AP was made up as a 1 M stock solution in deionized water. In experiments examining the effects of lowering intracellular pH on the block produced by 3-AP, the buffer 2-(*N*-morpholino)ethanesulfonic acid ($pK_a = 6.15$) was used.

Results

Inhibition of Kv1.1 channels by APs. Previous studies (14–16) have reported that Kv1.1 K^+ channels can be inhibited by 4-AP. However, the IC_{50} values for 4-AP block reported by those investigators range from 0.16 mM to 1 mM. Fig. 1A shows the concentration-dependent reduction in the outward current elicited by 4-AP in Sol-8 cells with either a 50-msec or 500-msec depolarizing pulse to +40 mV. It can be noted that the current traces recorded at high 4-AP concentrations (i.e., equal to or greater than 0.3 mM) exhibited a small, time-dependent increase in amplitude, relative to control, during the depolarizing pulse. The reason for this phenomenon is unclear; however, a similar phenomenon has been shown in previous reports of 4-AP block of Kv1.2 (23) and Kv2.1 (12) channels. Fig. 1B shows the dose-response relationship for 4-AP block of Kv1.1 currents in Sol-8 cells. For the purposes of this study we chose to derive estimates of block by measuring both the current amplitude at the end of a 50-msec depolarizing pulse to +40 mV and the tail current amplitude after repolarization to −60 mV. The tail current analysis was performed to ascertain whether the outward current measured at +40 mV was contaminated with the time-independent outward current that was evident upon establishment of the whole-cell configuration (see Materials and Methods). Before its run-down, this time-independent current contributed up to 15% of the total outward current; however, in contrast to Kv1.1, this current exhibited no measurable tail current. As can be seen in Fig. 1B, the similarity between the two dose-response curves indicates that there was little or no contribution of the time-independent current in the dose-response measurements. The concentration dependence of the inhibition by 4-AP exhibited a Hill coefficient of 0.91, which was deemed sufficiently close to unity to allow fitting of the data to a Langmuir isotherm, with a fitted half-maximal blocking concentration (IC_{50}) of 88 ± 5 μM ($n = 9$). Because of the small time-dependent changes in current amplitude that occur in the presence of 4-AP, the IC_{50} should be considered as representing quasi-steady state block.

Relationship between block and channel activation. After the application of 0.3 mM 4-AP to Sol-8 cells, it was noted that voltage steps applied within 10–15 sec elicited outward currents that were slightly reduced in amplitude but exhibited a clear decay phase that was absent in control records (Fig. 2A). Subsequent voltage steps applied at 15-sec intervals evoked outward currents that exhibited successively less decay,

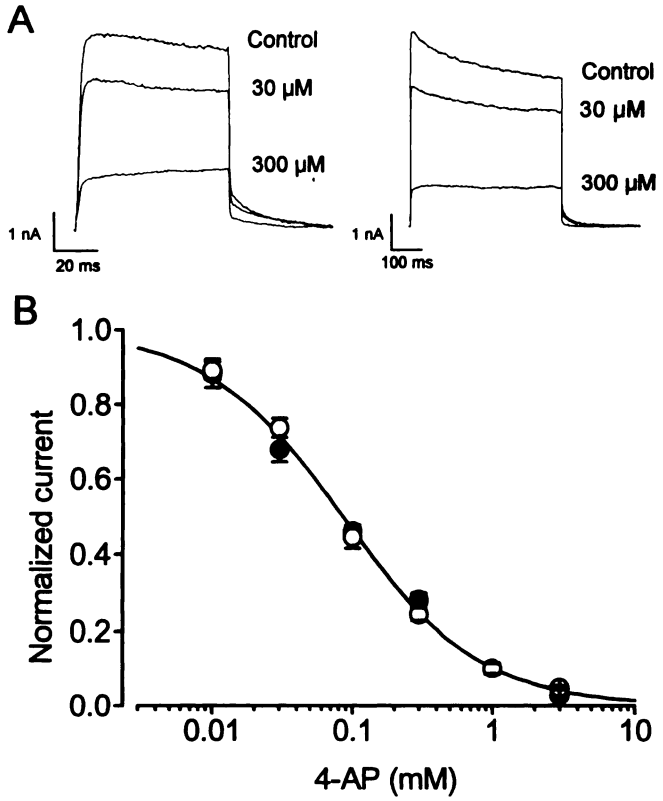

Fig. 1. Concentration-dependent inhibition of Kv1.1 K^+ currents by 4-AP in Sol-8 cells. A, Superimposed family of current traces showing inhibition produced by 30 μM and 300 μM 4-AP. Development of block at each concentration was monitored by application of either a 50-msec (*left*) or 500-msec (*right*) voltage step to +40 mV every 15 sec, from a holding potential of −80 mV, followed by repolarization to −60 mV until no further reduction in current amplitude was observed. The current traces show maximal inhibition achieved at each concentration of 4-AP. The two sets of current traces were obtained from separate cells. B, Dose-response curve of 4-AP-induced inhibition. Inhibition was assessed by measuring both the current amplitude at the end of a 50-msec depolarizing pulse to +40 mV (○) and the peak tail current amplitude after repolarization to −60 mV (●) and normalizing them with respect to the control value. The *curve* is a nonlinear least squares fit of a Langmuir isotherm to the data, using an IC_{50} of 88 μM. *Data points* are means of nine observations. *Standard error bars* are shown where they exceed the size of the symbol.

until by the fourth pulse (1 min), at which point steady state block had been achieved, current decay was again absent. Upon washout of the drug, current amplitude, monitored by voltage steps applied every 15 sec, increased to control levels within 5–10 min.

The appearance of a decay phase of Kv1.1 currents after the initial application of 4-AP suggested that the drug either induced an inactivation process that was absent under control conditions or, perhaps, evoked a time-dependent block of open Kv1.1 channels similar to that reported for 4-AP block of inactivating K^+ currents in GH_3 cells (11). A consistent feature of the onset of block by 4-AP was the finding that the peak current amplitude of successive current sweeps was similar to the current amplitude at the end of the preceding current sweep (Fig. 2A). This finding suggested that little or no block occurred between successive current sweeps (i.e., no block occurred when the channel was closed). To examine the possibility that 4-AP block required channel activation, the following pulse protocol was applied. The membrane potential was initially held at −80 mV (to populate the closed channel state). 4-AP (0.3 mM) was

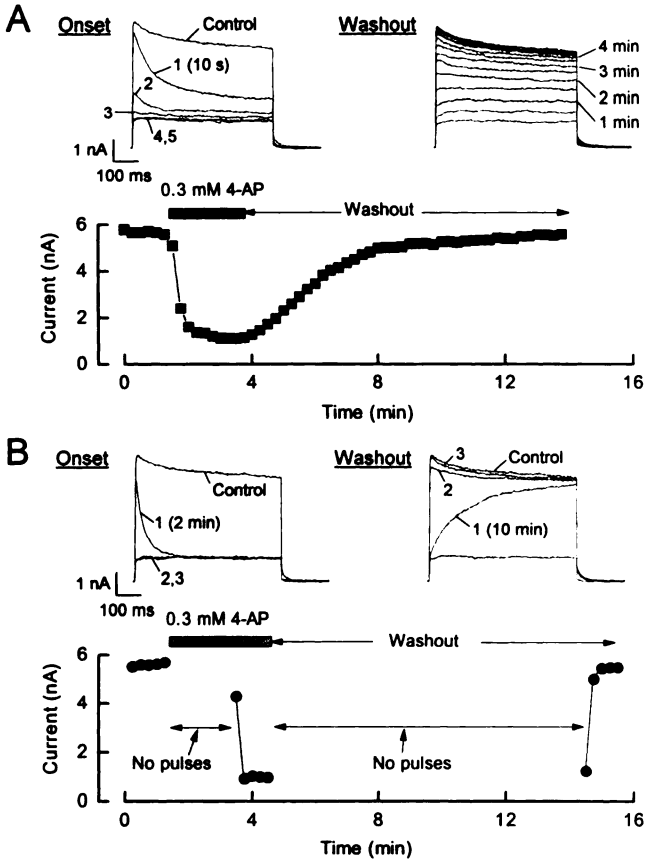

Fig. 2. Requirement of channel activation for block and unblock by 4-AP in Sol-8 cells. A, Development and washout of block of Kv1.1 K^+ currents after exposure to 0.3 mM 4-AP. Sequential 500-msec voltage steps to +40 mV (from a holding potential of −80 mV) were applied every 15 sec to assess changes in current amplitude. *Upper, left*, current traces elicited by the first five voltage steps (*1-5*) after application of 4-AP, along with the control current; *right*, washout of 4-AP (current traces elicited by alternate voltage steps, i.e., every 30 sec, are shown). *Lower*, complete time course for block and unblock by 0.3 mM 4-AP. B, Development of block and unblock of Kv1.1 K^+ currents after exposure to 0.3 mM 4-AP in the absence of channel opening. Current traces were elicited by the same pulse protocol as in A. *Upper, left, current trace 1* was generated after a 2-min exposure to 4-AP at −80 mV; *current traces 2* and *3* were elicited 15 sec and 30 sec, respectively, after *trace 1*, in the continued presence of 4-AP. *Right, current trace 1* was elicited after a 10-min washout of 4-AP at a holding potential of −80 mV (*unlabeled current trace*, maximal level of block produced by 4-AP); *current traces 2* and *3* were evoked 15 sec and 30 sec, respectively, after *trace 1*. The control current obtained before 4-AP application is shown for comparison. *Lower*, the complete time course for block and unblock under the aforementioned conditions. The data presented in A and B are from the same cell.

then applied for 2 min at this potential in the absence of activating voltage steps. Based on the results shown in Fig. 2A, a 2-min exposure should be sufficient for the drug concentration to reach steady state at or near its site of interaction. After the 2-min quiescent exposure period, 500-msec depolarizing voltage steps to +40 mV were applied every 15 sec in the continued presence of 4-AP, to assess the degree of inhibition. Fig. 2B (*current traces in left panel*) shows that the current elicited by the first depolarizing voltage step after the 2-min exposure to 4-AP exhibited a small initial reduction in peak amplitude, followed by a marked time-dependent decline in current amplitude to a level that approximated the steady state inhibition seen in Fig. 2A. The second and third depolarizing voltage steps, applied 15 and 30 sec, respectively, after the first pulse, elicited nondecaying currents with amplitudes identical to the current level observed at the end of the first voltage step. These results suggest that before the first depolarizing voltage step there had been little or no block of the channel. However, upon channel activation 4-AP bound in an exponential manner until steady state was reached, ~250 msec after the beginning of the depolarizing pulse. No further block occurred with subsequent voltage steps. Further evidence for the time-dependent reduction in current amplitude being related to drug binding was provided by the observation that the rate of decay of the current was dependent on 4-AP concentration. Fig. 3 shows a linear relationship between the reciprocal of the time constant for the decay of current (τ_{block}) and 4-AP concentration. The data were fit to the following equation:

$$\tau_{block} = 1/([4\text{-AP}] \cdot k_{on} + k_{off}) \quad (1)$$

where k_{on} and k_{off} are the apparent association and dissociation rate constants, respectively. The least squares estimates were $5.5 \pm 0.1 \times 10^4$ M^{-1} sec^{-1} for k_{on} and 10.4 ± 0.4 sec^{-1} for k_{off}. These kinetic parameters were used to derive an apparent equilibrium dissociation constant K_d (k_{off}/k_{on}) of 188 μM, which is comparable to, although somewhat higher than, the IC_{50} determined from the dose-response curve in Fig. 1.

The results described above indicate that the channel may need to be activated before 4-AP can bind. This raises the question of whether the channel needs to be activated for 4-AP to unbind. To examine this possibility the following protocol was used. After steady state block with 0.3 mM 4-AP had been established, the membrane potential was clamped at −80 mV to maintain the channels in a closed state. The 4-AP was then washed out for 10 min. Based on the results presented in Fig. 2A, 10 min should be sufficient for complete washout of the blocking agent. The first depolarizing step after the washout period elicited a current whose initial magnitude was similar to that of the blocked current but increased exponentially during the 500-msec depolarization, to an amplitude just slightly less

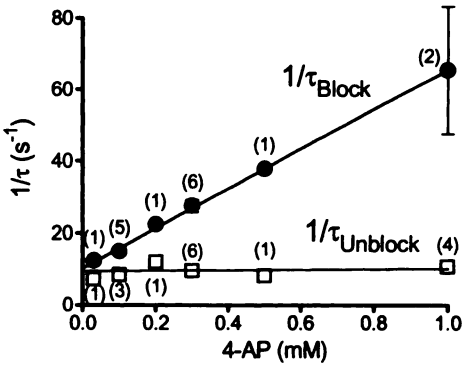

Fig. 3. Concentration dependence of the kinetics of 4-AP block and unblock of Kv1.1 currents in Sol-8 cells. A plot of the reciprocal of the time constants for block ($1/\tau_{block}$) (●) and unblock ($1/\tau_{unblock}$) (□) determined at different 4-AP concentrations is shown. The $1/\tau_{block}$ was derived from exponential fits to the decay phase of the first current trace elicited by a 500-msec voltage step to +40 mV after a 2-min exposure to 4-AP (see Fig. 2B). The value for $1/\tau_{unblock}$ was determined from exponential fits of the first current trace elicited after a 10-min washout of 4-AP in the absence of channel activation (see Fig. 2B for example). The *lines* are fits of eq. 1 to the data. The parameters used in the fit of $1/\tau_{block}$ are given in the text. *Numbers in parentheses*, numbers of data points at each concentration. Multiple data points for a given 4-AP concentration are shown as mean ± standard error (or range).

than that of the control current observed in the absence of drug (Fig. 2B, *right*). The second and third depolarizing voltage steps, applied 15 and 30 sec, respectively, after the first pulse, elicited currents with amplitudes and profiles similar to those of the control current. These results suggest that during the 10-min washout at −80 mV there was no unbinding of 4-AP (i.e., the drug was "trapped" within the closed channel). However, upon channel activation the drug dissociated. It is likely that the slow rising phase of the current elicited by the first pulse represents the rate of dissociation, because the time constant of the rising phase of the current (termed $\tau_{unblock}$) exhibited no dependence on the 4-AP concentration used to inhibit the current. The relationship between the reciprocal of $\tau_{unblock}$ and 4-AP concentration is shown in Fig. 3. The slope of the regression line fitted to these data did not differ significantly from 0 ($p > 0.17$). The mean reciprocal time constant for unblock ($1/\tau_{unblock}$) for all 4-AP concentrations examined was 9.7 ± 0.5 sec^{-1} ($n = 16$). This value is very similar to the estimate of k_{off} (equivalent to $1/\tau_{unblock}$) derived from a regression fit of $1/\tau_{block}$ in Fig. 3.

Voltage dependence of 4-AP block of Kv1.1 K^+ channels. Although 4-AP block and unblock of Kv1.1 K^+ channels occurred most readily after depolarizing voltage steps, an examination of the block at different membrane potentials indicated that the level of inhibition decreased at more depolarized potentials. Fig. 4A shows current traces elicited by a series of increasing depolarizing voltage steps in the absence and presence of 0.1 mM 4-AP. The current amplitude (measured at 50 msec) is plotted against membrane potential in Fig. 4B. In the presence of 4-AP there was a noticeable "plateau" phase in the current-voltage relationship between −30 mV and −20 mV (see current traces in Fig. 4A). When the relative availability of current in the presence of 4-AP is plotted as a function of membrane potential (Fig. 4C), it can be seen that the magnitude of inhibition increased as the membrane potential was depolarized from −40 to approximately −20 mV. However, further depolarization resulted in a reduction in block. The decline in 4-AP block was linear, decreasing by 20.5% over the potential range of −10 mV to +40 mV [slope of the line (0.0033 mV^{-1}) significantly different from 0; $p < 10^{-5}$]. The apparent increase in potency of 4-AP at potentials between −40 and −20 mV occurred over a range where the voltage dependence of steady state activation in the absence of drug was steepest. In contrast, the decline in 4-AP block at more depolarized voltages occurred at potentials at which channel activation in the absence of drug was >90% (see steady state activation curve in Fig. 4C).

The unblock of Kv1.1 K^+ channels induced by membrane depolarization to potentials greater than 0 mV is shown in Fig. 5. The cell was initially depolarized to 0 mV for 100 msec (from a holding potential of −80 mV) before stepping to successively more depolarized potentials for an additional 100 msec. In the absence of 4-AP, the initial depolarization to 0 mV elicited a rapidly activating outward current that exhibited no measurable inactivation over a period of 100 msec. Stepping the mem-

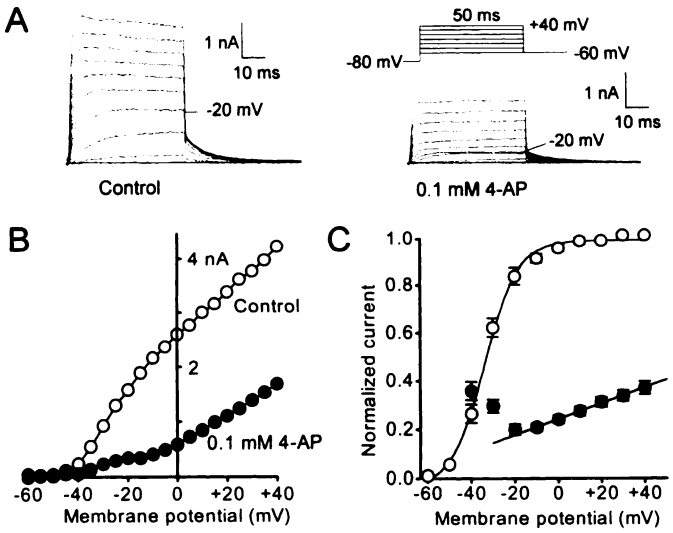

Fig. 4. Current-voltage relationship in the presence of 4-AP. A, Superimposed family of current sweeps elicited in Sol-8 cells by 50-msec voltage steps to potentials ranging from −60 mV to +40 mV, in the absence (*left*) and presence of 0.1 mM 4-AP (*right*). The current traces elicited by a pulse to −20 mV are labeled for comparison. B, Plot of current amplitude at the end of the 50-msec voltage step versus membrane potential in the absence (○) and presence (●) of 0.1 mM 4-AP (data obtained from current traces in A). C, Current availability in the presence of 0.1 mM 4-AP, plotted as amplitude versus membrane potential (●). Data were obtained from tail current amplitudes measured at −60 mV after 50-msec conditioning voltage steps. The data were normalized with respect to the estimated maximal current determined by a fit of a Boltzmann equation to the control tail current-voltage relationship (○). The fitted Boltzmann equation exhibited half-maximal activation at −33 ± 1 mV and a slope factor of 7 ± 1. The relationship between current availability in the presence of 4-AP and membrane potential over the voltage range of −10 mV to +40 mV was fitted by linear regression. The fitted slope was 0.0033 mV^{-1}, which is significantly different from 0 ($p < 10^{-5}$). Data are means ± standard errors from nine cells.

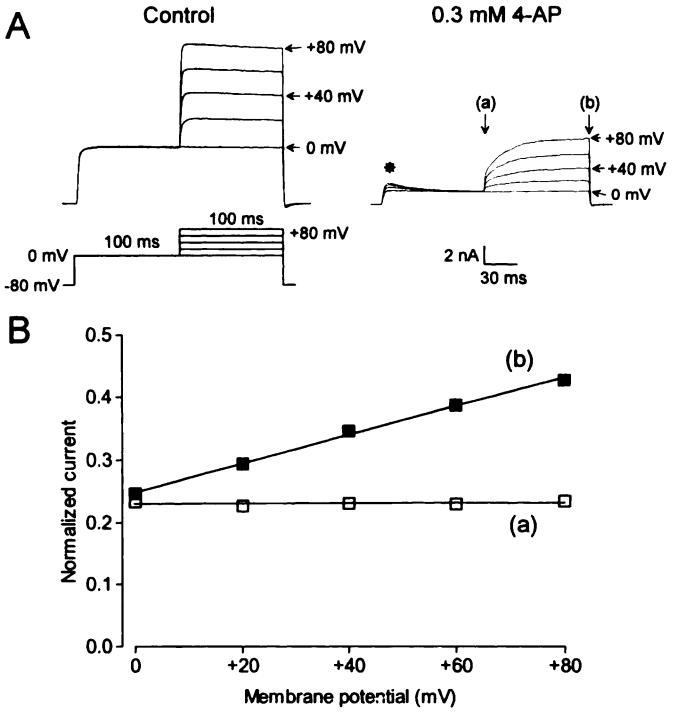

Fig. 5. Unblock of Kv1.1 channels in Sol-8 cells at depolarized potentials. A, Superimposed family of current traces elicited in the absence or presence of 0.3 mM 4-AP by a pulse protocol in which the membrane potential was stepped from −80 mV to 0 mV for 100 msec before stepping to potentials ranging from 0 mV to +80 mV for an additional 100 msec. B, Current amplitude at *point a* (□) and *point b* (■) in the family of current traces shown in A. Data have been normalized with respect to the current amplitudes at the same time points in the absence of 4-AP. See text for explanation of asterisk.

brane potential to consecutively more depolarized potentials resulted in additional outward current of successively greater magnitude that remained constant throughout the pulse. Currents elicited by the same pulse protocol in the presence of 0.3 mM 4-AP exhibited a different profile (Fig. 5A, *right*). The depolarizations from 0 mV to 20, 40, 60, and 80 mV in the presence of 4-AP elicited currents that exhibited an "instantaneous" jump followed by a slower exponential increase in current amplitude. Fig. 5B compares the degree of block that existed at the peak of the instantaneous current jump (Fig. 5A, *right, point a*) with the magnitude of block at the end of the pulse (Fig. 5A, *right, point b*). Although the magnitude of block at the beginning of the voltage step was similar at all potentials, inhibition at the end of the pulse declined with increasing depolarization. This result can be explained by assuming that the currents elicited by the various step depolarizations initially exhibit the same degree of block as that observed at 0 mV. However, during the maintained depolarization the magnitude of inhibition relaxes to a new equilibrium value that is defined by the change in affinity at the new membrane potential. The unblock that occurs during the step depolarizations to the various membrane potentials can also account for the appearance of larger decaying currents during the initial step depolarization to 0 mV (see asterisk in Fig. 5A) . For example, 4-AP that unbinds during the voltage step to +60 mV remains unbound when the membrane potential is returned to −80 mV at the end of the pulse (4-AP does not bind effectively to closed channels). The step depolarization to 0 mV in the following sweep activates unblocked channels that now have a relatively high affinity for 4-AP. These channels rebind 4-AP during the depolarization to 0 mV, thus giving rise to the decaying current.

To provide additional evidence that the voltage-dependent unblock at depolarized potentials was an intrinsic feature of Kv1.1 channels and not a property associated with the expression system, we also examined the effect of large membrane depolarizations on 4-AP block of Kv1.1 channels expressed in *Xenopus* oocytes (Fig. 6). *Xenopus* oocytes also have the advantage that they can withstand much larger depolarizing voltage steps than Sol-8 cells, and thus it was possible to examine the voltage dependence of block over a wider range of membrane potentials. As seen in Sol-8 cells, 4-AP block of Kv1.1 channels expressed in *Xenopus* oocytes appeared to require channel activation. Furthermore, 4-AP could be trapped upon channel closure. It was evident that the apparent potency of 4-AP block in *Xenopus* oocytes seemed to be less than in Sol-8 cells. The reason for this is unclear; however, it may reflect problems in drug equilibration across the viteline and plasma membranes and within the relatively large intracellular volume of distribution (IC_{50} values ranging from 0.16 to 1 mM have been reported for 4-AP block of Kv1.1 expressed in oocytes) (14, 15).

We took advantage of the 4-AP trapping phenomenon to examine the voltage dependence of block in oocytes. Using a variation of the pulse protocol used in Fig. 5, oocytes were initially depolarized for 600 msec to membrane potentials ranging from 0 mV to +140 mV. The membrane potential was then repolarized to −80 mV for 100 msec before application of a 600-msec depolarizing test voltage step to 0 mV to assess the degree of unblock. In the absence of 4-AP, currents elicited by the test pulse remained constant in amplitude. However, in the presence of 1 mM 4-AP, conditioning pulses to potentials greater than 0 mV resulted in test pulse currents that exhibited an inactivating

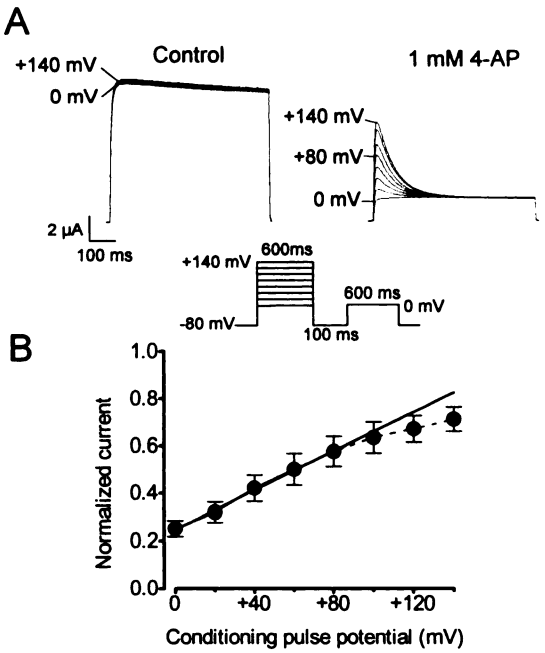

Fig. 6. Voltage dependence of 4-AP inhibition of Kv1.1 currents expressed in *Xenopus* oocytes. A, Superimposed family of current traces elicited in the absence or presence of 1 mM 4-AP by a 600-msec voltage step to 0 mV. This test pulse was preceded by a 600-msec conditioning depolarizing pulse to potentials ranging from 0 mV to +140 mV. B, Plot of peak test pulse current amplitude versus conditioning pulse potential determined in the presence of 1 mM 4-AP. Data have been normalized with respect to test pulse current amplitude measured in the absence of drug. The relationship between current availability in the the presence of 4-AP and membrane potential over the voltage range of 0 mV to +80 mV was fitted by linear regression. The fitted slope was 0.0041 ± 0.0001 mV^{-1}, which is significantly different from 0 ($p < 10^{-4}$). *Data points* are means ± standard errors from five oocytes.

component that increased in magnitude as the conditioning pulse was made more depolarized (Fig. 6A). The amplitude of the inactivating current component almost certainly represents the fraction of channels that became unbound during the conditioning pulse. The decay of the current likely reflects the time course of reblock of these channels at 0 mV, because both the steady state current level (i.e., at the end of the 600-msec test pulse) and the time constant for current decay remained constant irrespective of the conditioning pulse voltage. Fig. 6B shows that, over the voltage range of 0 mV to +80 mV, the decline in block by 1 mM 4-AP decreased linearly, exhibiting a slope of 0.0042 mV^{-1} (significantly greater than 0, $p < 10^{-4}$), which is similar to the slope of the voltage dependence of 4-AP block in Sol-8 cells. The reason for the deviation from linearity at potentials more positive than +100 mV is not clear and has not been examined further.

Slow block by 4-AP at hyperpolarized potentials. Although Fig. 2 showed that a 2-min exposure to 4-AP in the absence of channel activation produced only a small degree of inhibition at the beginning of the first depolarizing voltage step, it was found that increasing the time of exposure to 4-AP before the first activating voltage pulse resulted in a greater degree of block. Fig. 7A shows a series of current traces obtained from cells that had been exposed to 0.3 mM 4-AP for either 1 min or 10 min before the application of the first depolarizing voltage step. After a 1-min exposure to the drug, the peak current amplitude of the first pulse was reduced by 10% (ex-

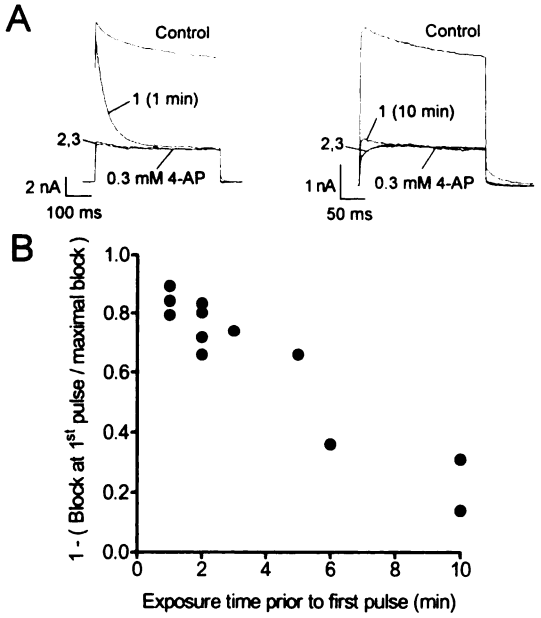

Fig. 7. Slow development of block by 4-AP at hyperpolarized potentials in Sol-8 cells. A, Family of consecutive current sweeps showing the development of block after a 1-min (*left*) or 10-min (*right*) exposure to 0.3 mM 4-AP, at a maintained holding potential of −80 mV. *Current traces 1* were elicited by a 500-msec voltage step to +40 mV and show the extent of block at the end of this initial phase of exposure. *Current traces 2* and *3* were elicited 15 sec and 30 sec, respectively, after *trace 1*, in the continued presence of 4-AP. B, Plot of the time-dependent reduction in peak amplitude of the current elicited by the first depolarizing voltage step after exposure to 0.3 mM 4-AP at −80 mV. The reduction in peak current amplitude has been normalized with respect to the maximal level of block (peak amplitude of current elicited by the third voltage step) (see A, *trace 3*). Each *data point* is from a separate cell.

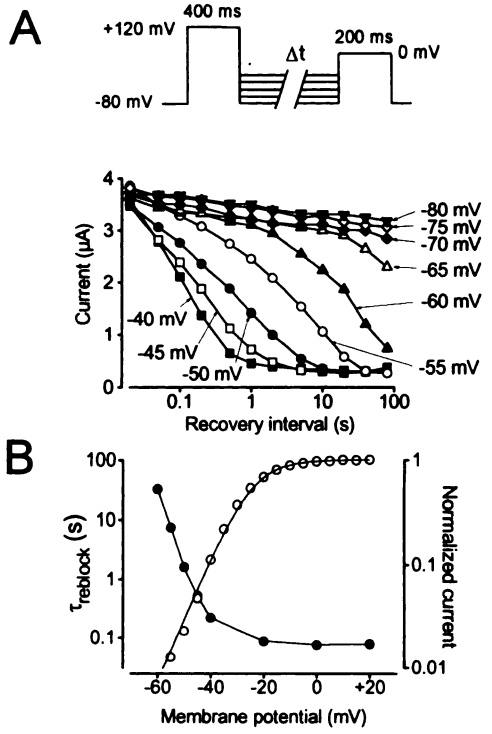

Fig. 8. Kinetics of 4-AP block of Kv1.1 currents expressed in *Xenopus* oocytes at hyperpolarized membrane potentials. A, Time course of reblock by 4-AP at different membrane potentials. A fraction of bound 4-AP was initially displaced by a 400-msec conditioning depolarization to +120 mV. The oocyte was then repolarized to various membrane potentials (ranging from −80 mV to −40 mV) for increasing durations before measurement of the current amplitude 15 msec after commencement of a 200-msec test pulse to 0 mV, to assess the degree of reblock. Note that the time course for reblock is plotted on a logarithmic scale. B, Plot of the voltage dependence of the time constant for reblock ($\tau_{reblock}$) (●). Also shown is the steady state activation curve for Kv1.1 in *Xenopus* oocytes (derived from tail currents elicited at −60 mV after 150-msec depolarizations to various potentials) (○). The *curve* is a fit of a Boltzmann equation with an estimated midpoint potential of activation of −26 mV and a slope factor of 7. Note that the *y*-axes have logarithmic scales.

pressed as a percentage of the maximal steady state reduction in current) (see Fig. 7A, *current trace 2*). In contrast, an 85% reduction was observed after a 10-min exposure to 4-AP. The time course for the onset of inhibition by 0.3 mM 4-AP at −80 mV is summarized in Fig. 7B. Half-maximal inhibition occurred at approximately 6 min.

To examine more closely the interaction of 4-AP with Kv1.1 channels at or below the apparent threshold potential for channel activation (i.e., −45 mV) (see Fig. 4), we again took advantage of the fact that 4-AP could be displaced from its binding site by large depolarizations. *Xenopus* oocytes expressing Kv1.1 channels were initially depolarized to +120 mV for 400 msec to displace a fraction of the bound 4-AP. The membrane potential was then repolarized, to potentials ranging from −80 mV to −40 mV, for various periods before application of a test pulse to 0 mV to assess the degree of reblock. A similar protocol has been previously used to examine the kinetics of AP block of the squid axon delayed rectifier K^+ channel at hyperpolarized holding potentials (24). Fig. 8A shows the time course of reblock at membrane potentials ranging from −80 mV to −40 mV. The time constants for reblock ($\tau_{reblock}$) at these potentials are plotted in Fig. 8B, along with $\tau_{reblock}$ at −20 mV, 0 mV, and +20 mV derived from the decay of the inactivating current component elicited at these potentials after a 400-msec conditioning pulse to +120 mV. Also shown in Fig. 8B is the steady state activation curve for Kv1.1 in *Xenopus* oocytes. It can be seen that the biggest changes in $\tau_{reblock}$ occurred over the membrane potential range of −60 mV to −40 mV. The $\tau_{reblock}$ decreased by a factor of 150, from 33 sec at −60 mV to 0.2 sec at −40 mV. In contrast, $\tau_{reblock}$ declined by a factor of only 2.5 between −40 mV and +20 mV. A comparison of the voltage dependences of $\tau_{reblock}$ and open channel probability (P_{open}, estimated from a fit of the Boltzmann equation to the steady state activation curve) indicates that the decrease in the rate of reblock is correlated with reduced availability of open channels, especially when P_{open} falls below 0.1 (which occurs at approximately −40 mV). It should be noted that Kv1.1 channels were found to exhibit slow inactivation at −40 mV (also see Ref. 13). However, the time constant for inactivation (τ = 23 sec) was 100-fold slower than the rate of reblock and thus is unlikely to influence the measurement. No inactivation was evident at −60 mV for durations of up to 80 sec.

Block of Kv1.1 K^+ channels by 3-AP. Several studies examining 4-AP block of K^+ channels in a variety of cell types have concluded that access to the site of block is from the intracellular face and that the charged form of the blocker is active (8, 12, 25, 26). Indeed, at physiological pH (i.e., ~7.2) 99% of 4-AP exists in the charged form (4-AP pK_a = 9.2). It is possible to speculate that the charged form of 4-AP can gain access to, or egress from, its binding site only via the hydrophilic aqueous pathway. This pathway may be available only when

the channel activates. To examine the possibility that uncharged AP may be able to reach its binding site in the absence of channel activation, possibly via a hydrophobic pathway, the blocking effect of 3-AP on Kv1.1 K^+ currents was examined. 3-AP is an isomer of 4-AP that has a pK_a of 6.0. Therefore, at physiological pH approximately 94% of 3-AP is in the neutral form. 3-AP was found to block Kv1.1 K^+ currents. However, it was approximately 20-fold less potent than 4-AP. Nevertheless, 3-AP was found to bind and unbind most readily after channel activation (Fig. 9). Fig. 9A shows that, after rapid exposure to 10 mM 3-AP, application of a voltage step within 10 sec elicited an outward current that decayed to a steady state level of block within 200 msec. Reversal of block was similarly rapid upon washout of the drug, with complete reversal being achieved after five consecutive voltage steps to +40 mV applied every 15 sec (total washout time, 75 sec). Fig. 9B shows that, after a 1-min exposure to 10 mM 3-AP in the absence of channel activation, the current elicited by the first depolarizing voltage step exhibited a small initial reduction in peak amplitude, followed by a marked time-dependent decline in current amplitude to a level that approximated the steady state inhibition seen in Fig. 9A. The second and third depolarizing voltage steps, applied 15 and 30 sec, respectively, after the first pulse, elicited nondecaying currents with amplitudes identical to the current level observed at the end of the first voltage step. These results indicate that before the first depolarizing voltage step there was little or no block of the channel. However, upon channel activation the 3-AP bound in an exponential manner until steady state was reached. After steady state block with 10 mM 3-AP had been established, the membrane potential was clamped at −80 mV to maintain the channels in a closed state. The 3-AP was then washed out for 5 min. The first depolarizing step after the washout period elicited a current whose initial magnitude was similar to that of the blocked current but increased exponentially during the 500-msec depolarization, to an amplitude just slightly less than that of the control current observed in the absence of drug. The second and third depolarizing voltage steps, applied 15 and 30 sec, respectively, after the first pulse, elicited currents with amplitudes and profiles similar to those of the control current. The time constant of the unblock that occurred during the first voltage step was found to be independent of 3-AP concentration. The mean $\tau_{unblock}$ was 86 ± 9 msec (n = 5). This is very similar to the value obtained for 4-AP (109 msec).

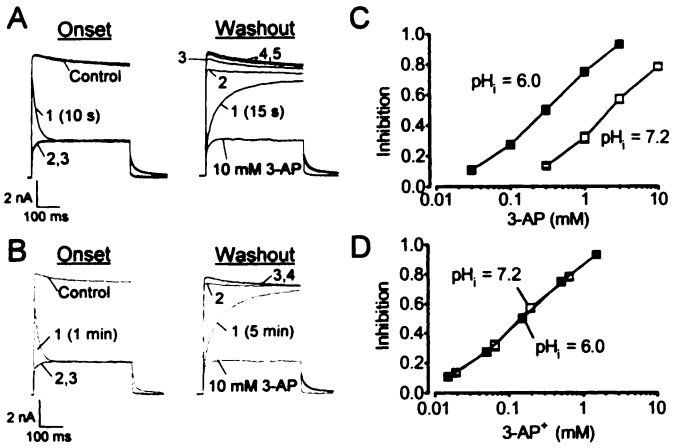

Fig. 9. Block of Kv1.1 currents by 3-AP. A, Development and washout of block of Kv1.1 K^+ currents in Sol-8 cells after exposure to 10 mM 3-AP, using the same pulse protocol as in Fig. 2. Sequential 500-msec voltage steps to +40 mV (from a holding potential of −80 mV) were applied every 15 sec, to assess changes in current amplitude. *Left*, current traces elicited by the first three voltage steps (*1*, *2*, and *3*) after application of 3-AP, along with the control current. *Right*, washout of 3-AP. B, Development of block and unblock of Kv1.1 K^+ currents after exposure to 10 mM 3-AP in the absence of channel opening. Current traces were elicited by the same pulse protocol as in A. *Left*, *current trace 1* was generated after a 1-min exposure to 3-AP at −80 mV; *current traces 2* and *3* were elicited 15 sec and 30 sec, respectively, after *trace 1*, in the continued presence of 3-AP. *Right*, *current trace 1* was elicited after a 5-min washout of 3-AP at a holding potential of −80 mV; *current traces 2*, *3*, and *4* were evoked 15 sec, 30 sec, and 45 sec, respectively, after *trace 1*. The data presented in A and B are from the same cell. C, Dose-response curve of 3-AP-induced inhibition of Kv1.1 K^+ currents in Sol-8 cells at intracellular pH values of 6.0 (■) and 7.2 (□). Inhibition was assessed by measuring current amplitude at the end of the voltage step to +40 mV and normalizing it with respect to the maximal block. The IC_{50} was 2.2 mM at pH 7.2 and 0.29 mM at pH 6.0. *Data points* are means of three to five cells at pH 7.2 and nine cells at pH 6.0. *Standard error bars* are shown where they exceed the size of the symbol. D, Dose-response curve for the inhibition of Kv1.1 K^+ currents by the charged form of 3-AP at intracellular pH values of 6.0 and 7.2. The data are the same as in C. The concentration of the charged form of 3-AP was calculated assuming a pK_a of 6.03. The IC_{50} for the charged form of 3-AP was 140 μM and 145 μM at pH 7.2 and 6.0, respectively.

Despite its low potency, 3-AP exhibits a blocking profile similar to that of 4-AP. One possible explanation for these observations is that the neutral form of the APs has a lower affinity than the charged form for the site of interaction on the channel. However, one would have to assume that the reduced affinity results from a much slower association rate constant, because the dissociation rate constants ($1/\tau_{unblock}$) for 3-AP and 4-AP were similar. An alternative explanation is that the charged form of 3-AP is the active form. If this is true then one would expect that, by increasing the proportion of 3-AP existing in the charged form, the apparent potency would be increased. Fig. 9C shows dose-response curves obtained with 3-AP at intracellular pH values of 7.2 and 6.0. Under these conditions 6% and 50%, respectively, of the intracellular 3-AP is in the charged from. At pH 7.2 the IC_{50} for 3-AP was 2.2 ± 0.4 mM, whereas at pH 6.0 the IC_{50} was 0.29 ± 0.02 mM. Fig. 9D shows dose-response curves at both pH values, assuming that only the charged form of 3-AP is active. Under these conditions the IC_{50} values at pH 7.2 and 6.0 were very similar, being 140 μM and 145 μM, respectively. These values are similar to the IC_{50} for 4-AP. These results are consistent with drug access to the blocking site being from the intracellular side of the channel.

Lack of effect of extracellular K^+ concentration elevation on inhibition of Kv1.1 channels by 4-AP. The observation that 4-AP interacts most readily with activated channels raises the question of whether the 4-AP binding site is within the permeation pathway. A widely used test for occlusion of the K^+ channel pore by a blocking ion at an internal site is to determine whether elevation of the extracellular K^+ concentration can relieve the block. For example, Armstrong (27) showed that, in the presence of elevated extracellular K^+ concentrations, intracellular application of tetraethylammonium in squid giant axon blocked outward currents through the delayed rectifier more effectively than inward currents. The effect of elevation of extracellular K^+ concentrations on steady state inhibition of Kv1.1 currents by 4-AP is shown in Fig. 10A. The magnitude of inhibition by 0.1 mM 4-AP was determined from currents elicited by voltage steps to −20 mV in

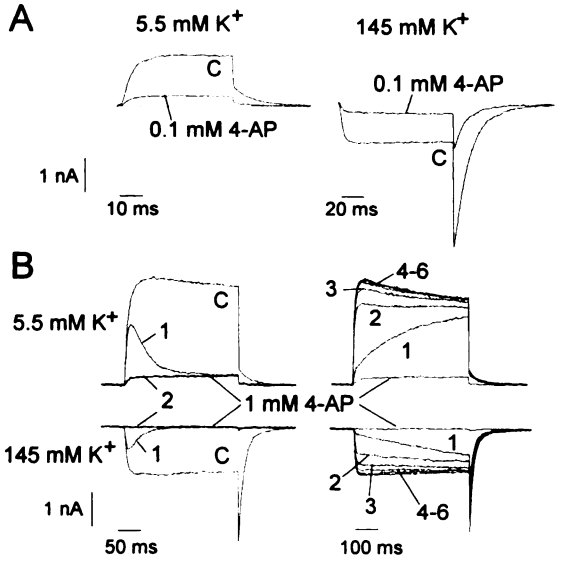

Fig. 10. Lack of effect of increases in extracellular K^+ concentration on block of Kv1.1 currents in Sol-8 cells by 4-AP. A, Superimposed current traces recorded in the absence (*C*) and presence of 0.1 mM 4-AP in extracellular bathing solutions containing either 5.5 mM K^+ or 145 mM K^+. Currents were elicited by depolarizing voltage steps from −80 mV to −20 mV. Tail currents were evoked by repolarization to −60 mV in 5.5 mM K^+ or −80 mV in 145 mM K^+. B, Development and washout of block of Kv1.1 K^+ currents after exposure to 1 mM 4-AP in the presence of 5.5 mM K^+ or 145 mM K^+, using the same pulse protocol as in Fig. 2. Sequential 250-msec or 500-msec voltage steps to −30 mV (from a holding potential of −80 mV) were applied every 15 sec, to assess changes in current amplitude. *Left*, *current traces 1* were generated after a 2-min exposure to 4-AP at −80 mV; *current trace 2* was elicited 15 sec after *trace 1*, in the continued presence of 4-AP. *Right*, *current traces 1* were elicited after a 10-min washout of 4-AP, at a holding potential of −80 mV; *current traces 2* through *6* were evoked at 15-sec intervals after *trace 1*. The data presented for 5.5 mM K^+ and 145 mM K^+ are from the same cell.

extracellular bathing solutions containing either 5.5 mM or 145 mM K^+. Examination of the inhibition at a fixed potential prevented voltage-dependent changes in 4-AP binding affinity from contributing to differences in the magnitude of inhibition. It can be seen in Fig. 10A that under these conditions elevation of the extracellular K^+ concentration from 5.5 mM to 145 mM had a negligible effect on the magnitude of inhibition by 4-AP. Steady state inhibition was 78% in 5.5 mM K^+ and 72% in 145 mM K^+. A similar lack of effect of K^+ concentration on steady state inhibition was observed in three other cells.

Additional evidence for a lack of effect of increases in the extracellular K^+ concentration on the block produced by 4-AP is shown in Fig. 10B. In this particular experiment, block by 1 mM 4-AP in 145 mM K^+ was 100%, which was even more complete than that in 5 mM K^+ (~95%). The apparent rate of block upon channel activation, and the rate of unblock from the activated channel after washout of the drug at −30 mV, remained essentially unchanged when the extracellular K^+ concentration was elevated from 5.5 mM to 145 mM. A similar result was also observed at +40 mV (data not shown). It can be noted that the apparent rate of dissociation of 4-AP after washout of the drug at −30 mV was slower than at +40 mV (see Fig. 2). This may reflect a higher affinity of the channel for 4-AP at −30 mV, compared with +40 mV. However, the differences may also result from the fact that at −30 mV the open probability for the channel is ~0.5 (estimated from steady state activation curves), compared with ~1 at +40 mV. If unblock occurs only from open channels, it is possible to predict that, during fixed-duration voltage steps, 4-AP has on average less time to unbind at −30 mV than at +40 mV, due to the lower proportion of time spent in the open state.

Discussion

The results presented in this study indicate that the interaction of APs with Kv1.1 K^+ channels expressed in *Xenopus* oocytes or the mammalian Sol-8 cell line involves a complicated interplay between membrane potential, channel gating, and the form of the drug present.

Relationship between AP block and channel gating. Results obtained in this study lead us to conclude that APs block Kv1.1 K^+ channels most readily during channel activation. Short applications (10–15 sec) of 4-AP and 3-AP result in the appearance of current decay that is not present in the absence of the blocker. This phenomenon can be explained by 4-AP producing a time-dependent block of open channels, similar in nature to 4-AP block of transient outward K^+ channels in GH_3 cells (11). A preferential interaction of APs with activated channels is reflected by the finding that, even when the resting closed channel is exposed to 4-AP for a period of time sufficient for drug levels to reach steady state (1–2 min), little or no initial reduction in current amplitude is evident after a depolarizing pulse to +40 mV. However, during the voltage pulse the current decays exponentially to a level that is maintained throughout the duration of 4-AP exposure. These results, which are similar to reported actions of 4-AP on transiently activated K^+ currents in lymphocytes and GH_3 cells (8, 11) and, more recently, on the cloned delayed rectifier K^+ channels Kv2.1 and Kv3.1 (12), suggest that, under the conditions described above, 4-AP binds preferentially to the open state of the channel.

In addition to showing the importance of channel activation for AP block, the present study has shown that unbinding of APs from Kv1.1 channels also appears to require channel activation. The clearest evidence for this comes from the finding that, after washout of the blocker, no unblock occurs until the channel is activated by membrane depolarization. Thus, 4-AP can be trapped within the channel when it closes. Choquet and Korn (8) have reported a similar trapping of 4-AP after closure of transiently activated K^+ currents in lymphocytes.

A significant level of inhibition was found to develop when channels were held at hyperpolarized potentials (i.e., −80 mV) after exposure to 4-AP for longer durations (up to 10 min). One explanation for this phenomenon is that 4-AP can access its binding site when the channel is in a closed rested state but at a much slower rate ($t_{1/2}$ for block, ~5 min at 0.3 mM) than occurs after channel activation (τ_{block}, 37 msec at 0.3 mM). A similar explanation has recently been used to account for the slow block of Kv2.1 and Kv3.1 K^+ channels by 4-AP (12). An alternative explanation is that the channel can still open at hyperpolarized potentials and 4-AP interacts with short-lived open channels. Based on the kinetic model of RCK1 activation proposed by Koren *et al.* (13), the calculated probability of channel opening at −80 mV is 0.02% and the mean open channel lifetime is ~250 μsec. Thus, over a period of 10 min the channel would be predicted to be open for a total of 120 msec. In the present study, kinetic evidence that favors an interaction of 4-AP with open channels at hyperpolarized po-

tentials was provided by the observation that the voltage dependence of the time constant for block at potentials near the apparent threshold for current activation (i.e., approximately −45 mV) correlated well with the estimated open channel probability (P_{open}) at these potentials (Fig. 7). The apparent rate of block by 1 mM 4-AP decreased by a factor of 150, from 4.5 sec^{-1} at −40 mV (P_{open}, ~0.12) to 0.03 sec^{-1} at −60 mV (P_{open}, ~0.008). It is worth noting, however, that the aforementioned kinetic data do not exclude the possibility that APs may interact with one or more of the closed gating states through which the channel passes during channel activation. Using a protocol similar to the one described above to monitor the kinetics of AP reblock of delayed rectifier K^+ currents in squid axons, Kirsch *et al.* (24) proposed that the availability of the AP binding site is modulated by channel gating, such that access is limited by the probability of the channel populating one or more intermediate closed states. A similar mechanism has been proposed to underlie 4-AP block of transiently activated K^+ currents in cardiac muscle (5, 6).

Voltage dependence of AP binding. Over the membrane potential range of −40 mV to −20 mV, the magnitude of block produced by 4-AP was found to increase as the cell was made more depolarized. In contrast, block by 4-AP decreased when the membrane potential was depolarized to potentials more positive than −20 mV. The apparent increase in potency between −40 mV and −20 mV coincided with the steepest part of the steady state activation curve observed in the absence of 4-AP. Because 4-AP block appears to require channel activation, it is likely that the apparent increase in potency reflects the increased availability of activated gating states at the more depolarized potentials. At potentials close to the apparent activation threshold, the channel open probability is low and consequently the probability that 4-AP is able to bind during a fixed-duration voltage step is also low. Similarly, because 4-AP appears to dissociate only from the activated channel, the apparent rate of dissociation might also be expected to be slower at potentials near the threshold. In agreement with these expectations, the time constants for block and unblock were found to be 2–3-fold slower at −30 mV than at +40 mV.

The decrease in 4-AP potency that occurred when the membrane potential was depolarized to potentials more positive than −10 mV agrees with similar findings describing 4-AP block of the delayed rectifier in nerve axons (2, 9) but contrasts with 4-AP block of I_{TO} in GH_3 cells (11) and block of the cloned delayed rectifier K^+ channels Kv2.1 and Kv3.1 expressed in *Xenopus* oocytes (12). The reduction in 4-AP potency at Kv1.1 K^+ channels occurred over a range of membrane potentials at which, in the absence of drug, channels are maximally activated. This would suggest that the voltage dependence of AP block over these potentials is not directly associated with the process of channel activation or that the voltage dependence of channel activation is modified by 4-AP. It is also possible that the voltage-dependent changes in channel conformation that underlie channel opening go beyond the structural configuration that permits the passage of K^+ ions. These additional conformational changes may modulate AP binding without affecting ion movement through the open channel.

The enhancing effect of lowered intracellular pH on the potency of block induced by 3-AP indicates that the charged form of the APs is the active species and that access to the binding site is probably from the intracellular face of the channel. However, the voltage dependence of AP block is opposite what would be expected for a charged drug moving through the membrane electrical field from the inside to block the open channel (this assumes that the binding site is within the electric field). For example, the open channel-blocking agents tetraethylammonium and quinidine (which are either completely or predominantly protonated at physiological pH values) have been shown to exhibit increases in potency with depolarization over a voltage range at which activation is maximal (27–30). Indeed, the similarity in the voltage dependence of block by tetraethylammonium and quinidine has led to speculation that the binding sites for these agents may be the same or in close proximity (30). At present there is only limited structural information concerning the location of the 4-AP binding site on K^+ channels. Site-directed mutation analysis and construction of chimeric K^+ channels indicate that, at least for Kv3.1 K^+ channels (31), the 4-AP binding site is located within the cytoplasmic mouth of the permeation pathway but lies outside the membrane electric field (as indicated by the apparent absence of voltage-dependent block) (12). The pattern of the voltage dependence of 4-AP block of Kv1.1 channels observed in this study prevents any clear conclusions from being drawn concerning the position of the AP binding site with respect to the membrane electric field. However, if the binding site does lie within the membrane electric field, then the full magnitude of the decrease in potency of 4-AP observed with depolarization may actually be attenuated.

The present study has shown that the magnitude and kinetics of block of Kv1.1 channels by 4-AP are not modulated by elevation of extracellular K^+ concentration. These results are consistent with previous reports of little or no effect of extracellular K^+ concentration on 4-AP inhibition of the delayed rectifier K^+ current in squid giant axons (2, 9). However, the lack of effect of increasing the extracellular K^+ concentration contrasts with the attenuating effect that such a procedure has on the magnitude of inhibition of delayed rectifier K^+ currents by open channel-blocking agents, such as intracellularly applied tetraethylammonium (27, 32). Although the ability of a permeant ion to modulate the blocking action of a drug is often used as evidence of occlusion of the conduction pathway, it is based on the assumption that the binding sites for the drug and the permeant ion are either the same or sufficiently close that electrostatic or allosteric interactions can reduce the binding of drug. However, it is also possible that a drug may bind to a site on the open channel that can prevent current flow but cannot sense occupancy of the conducting pathway by the permeant ion. Such a model has been proposed for the block of batrachotoxin-activated Na^+ channels by tetrodotoxin (33). A similar model may also account for the lack of effect of K^+ concentration on 4-AP block of Kv1.1 channels.

Conclusions. The present study has shown that block of Kv1.1 channels by APs requires channel activation. Furthermore, APs can be trapped after channel closure. The charged form of APs appears to be the active species, and access to the binding site seems to be via an intracellular pathway. The interaction of APs with Kv1.1 channels is voltage dependent. The affinity of the channel for 4-AP decreases as the membrane potential is made more depolarized.

References

1. Pelhate, M., and Y. Pichon. Selective inhibition of potassium currents in the giant axon of the cockroach. *J. Physiol. (Lond.)* **242**:90P (1974).
2. Yeh, J. Z., G. S. Oxford, C. H. Wu, and T. Narahashi. Dynamics of amino-

pyridine block of potassium channels in squid axon membrane. *J. Gen. Physiol.* **68**:519–535 (1976).
3. Gillespie, J. I., and O. F. Hutter. The actions of 4-aminopyridine on the delayed potassium current in skeletal muscle fibres. *J. Physiol. (Lond.)* **252**:70P–71P (1975).
4. Simurda, J., M. Simurdova, and G. Christe. Use-dependent effects of 4-aminopyridine on transient outward current in dog ventricular muscle. *Pfluegers Arch.* **415**:244–246 (1989).
5. Castle, N. A., and M. T. Slawsky. Characterization of 4-aminopyridine block of the transient outward K^+ current in adult rat ventricular myocytes. *J. Pharmacol. Exp. Ther.* **264**:1450–1459 (1993).
6. Campbell, D. L., Y. Qu, R. L. Rasmusson, and H. C. Strauss. The calcium-independent transient outward potassium current in isolated ferret right ventricular myocytes. II. Closed state reverse use-dependent block by 4-aminopyridine. *J. Gen. Physiol.* **101**:603–626 (1993).
7. Kehl, S. J. 4-Aminopyridine causes a voltage-dependent block of the transient outward K^+ current in rat melanotrophs. *J. Physiol. (Lond.)* **431**:515–528 (1990).
8. Choquet, D., and H. Korn. Mechanism of 4-aminopyridine action on voltage-gated potassium channels in lymphocytes. *J. Gen. Physiol.* **99**:217–240 (1992).
9. Ulbricht, W., and H. H. Wagner. Block of potassium channels of the nodal membrane by 4-aminopyridine and its partial removal on depolarization. *Pfluegers Arch.* **367**:77–87 (1976).
10. Thompson, S. Aminopyridine block of transient potassium current. *J. Gen. Physiol.* **80**:1–18 (1982).
11. Wagoner, P. K., and G. S. Oxford. Aminopyridines block an inactivating potassium current having slow recovery kinetics. *Biophys. J.* **58**:1481–1489 (1990).
12. Kirsch, G. E., and J. A. Drewe. Gating-dependent mechansim of 4-aminopyridine block in two related potassium channels. *J. Gen. Physiol.* **102**:797–816 (1993).
13. Koren, G., E. R. Liman, D. E. Logothetis, B. Nadal-Ginard, and P. Hess. Gating mechanism of a cloned potassium channel expressed in frog oocytes and mammalian cells. *Neuron* **2**:39–51 (1990).
14. Stuhmer, W., M. Stocker, B. Sakmann, P. Seeburg, A. Baumann, A. Grupe, and O. Pongs. Potassium channels expressed from rat brain cDNA have delayed rectifier properties. *FEBS Lett.* **242**:199–206 (1988).
15. Christie, M. J., J. P. Adelman, J. Douglass, and R. A. North. Expression of cloned rat brain potassium channel in *Xenopus* oocytes. *Science (Washington D. C.)* **244**:221–224 (1989).
16. Wang, S. Y., N. A. Castle, and G. K. Wang. Identification of RBK1 potassium channels in C6 astrocytoma cells. *Glia* **5**:146–153 (1992).
17. Castle, N. A., D. E. Logothetis, and G. K. Wang. 4-AP block of RCK1 K^+ currents expressed in Sol-8 cells: relationship between block and channel activation. *Biophys. J.* **64**:A197 (1993).
18. Hamill, O. P., A. Marty, E. Neher, B. Sakmann, and F. J. Sigworth. Improved patch-clamp techniques for high resolution current recording from cells and cell-free membrane patches. *Pfluegers Arch.* **391**:85–100 (1981).
19. Ravindran, A., L. Schild, and E. Moczydlowski. Divalent cation selectivity for external block of voltage-dependent Na^+ channels prolonged by batrachotoxin: Zn^{2+} induces discrete substates in cardiac Na^+ channels. *J. Gen. Physiol.* **97**:89–115 (1991).
20. Robbins, J., J. Trouslard, S. J. Marsh, and D. A. Brown. Kinetic and pharmacological properties of the M-current in rodent neuroblastoma × glioma hybrid cells. *J. Physiol. (Lond.)* **451**:159–185 (1992).
21. Harrison, N. L., H. K. Radke, M. M. Tamkun, and D. M. Lovinger. Modulation of gating of cloned rat and human K^+ channels by micromolar Zn^{2+}. *Mol. Pharmacol.* **43**:482–486 (1993).
22. Sim, J. A., and E. Cherubini. Submicromolar concentration of zinc irreversibly reduce a calcium dependent potassium current in rat hippocampal neurons *in vitro*. *Neuroscience* **36**:623–629 (1990).
23. Yamagishi, T., K. Ishii, and N. Taira. Absence of effects of class III antiarrhythmic agents on cloned cardiac K channels. *Jpn. J. Pharmacol.* **61**:371–373 (1993).
24. Kirsch, G. E., J. Z. Yeh, and G. S. Oxford. Modulation of aminopyridine block of potassium currents in squid axon. *Biophys. J.* **50**:637–644 (1986).
25. Kirsch, G. E., and T. Narahashi. Site of action and active form of aminopyridines in squid axon membranes. *J. Pharmacol. Exp. Ther.* **226**:174–179 (1983).
26. Howe, J. R., and J. M. Ritchie. On the active form of 4-aminopyridine: block of K^+ currents in rabbit Schwann cells. *J. Physiol. (Lond.)* **433**:183–205 (1991).
27. Armstrong, C. M. Interaction of tetraethylammonium ion derivatives with the potassium channels of giant axons. *J. Gen. Physiol.* **58**:413–437 (1971).
28. Kirsch, G. E., M. Taglialatela, and A. M. Brown. Internal and external TEA block in single cloned K^+ channels. *Am. J. Physiol.* **261**:C583–C590 (1991).
29. Yellen, G., M. E. Jurman, T. Abramson, and R. MacKinnon. Mutations affecting internal TEA blockade identify the probable pore-forming region of a K^+ channel. *Science (Washington D. C.)* **251**:939–942 (1991).
30. Snyders, D. J., K. M. Knoth, S. L. Roberds, and M. M. Tamkun. Time-, voltage-, and state-dependent block by quinidine of a cloned human cardiac potassium channel. *Mol. Pharmacol.* **41**:322–330 (1991).
31. Kirsch, G. E., C.-C. Shieh, J. A. Drewe, D. F. Vener, and A. M. Brown. Segmental exchanges define 4-aminopyridine binding and the inner mouth of K^+ pores. *Neuron* **11**:503–512 (1993).
32. Newland, C. F., J. P. Adelman, B. L. Tempel, and W. Almers. Repulsion between tetraethylammonium ions in cloned voltage-gated potassium channels. *Neuron* **8**:975–982 (1992).
33. Moczydlowski, E., S. S. Garber, and C. Miller. Batrachotoxin-activated Na^+ channels in planar lipid bilayers: competition of tetrodotoxin block by Na^+. *J. Gen. Physiol.* **84**:665–686 (1984).

Send reprint requests to: Neil A. Castle, Department of Anesthesia Research Laboratories, Brigham and Women's Hospital, 75 Francis Street, Boston, MA 02115.